Substitution Patterns in Mono-BN-Fullerenes: C_n (n = 20, 24, 28, 32, 36, and 40)

Jayasree Pattanayak, Tapas Kar,* and Steve Scheiner

Department of Chemistry and Biochemistry, Utah State University, Logan, Utah 84322-0300

Received: May 19, 2004

Semiempirical MNDO and Density Functional Theory (DFT) are applied to investigate the structure and properties of $C_{n-2}BN$ fullerenes, where n = 20, 24, 28, 32, 36, and 40. Low-mass fullerenes are of particular interest because of their high curvature and increased strain energy owing to adjacent pentagonal rings. The most important factor for stability is the connectedness of the heteroatoms. The BN group prefers to replace a short CC bond. N atoms tend toward smaller angles, leading them toward participation in pentagons over hexagons. The BN pair prefers hexagon−pentagon over pentagon−pentagon junctions. No systematic trends are observed in the effects of doping upon the HOMO-LUMO gap, ionization potential, and electron affinity. Whereas MNDO is unable to reliably predict the most stable isomers, single-point DFT calculations at MNDO-optimized geometries correctly reproduce the full DFT relative energy trends.

Introduction

The synthesis of low-mass fullerenes C_n (n < 60) on a macroscopic scale is an active field of current investigation**.** A number of smaller fullerenes C_n (n < 60) have been detected by mass spectroscopic methods[1] in the gas phase and numerous theoretical calculations have been performed to characterize them.[2−13] Kroto suggested that fullerenes C_n with magic numbers n = 24, 28, 32, 36, 50, 60, and 70 should have enhanced stability relative to those with similar numbers of atoms.[14]

In this family, C_{20} is the smallest possible fullerene[15] with no hexagonal rings. It contains just 12 pentagons, in a highly strained structure. The stable isomers of C_{20} clusters consist of bowl, ring, and fullerene (cage) structures, wherein fullerene (I_h) is the most stable.[15] Experimentally, each of these isomers can be produced under suitable reaction conditions.[1,16] Theoretical attempts to characterize C_{20} clusters have been reported by several groups.[4,5,17,18]

Similar structural alternatives arise for C_{24}, and the latest calculations indicate that D_6 symmetry is the most stable for C_{24}.[19−22] C_{28} was originally reported by Kroto in 1987[14] and the tetrahedral symmetry of C_{28} was shown to be the most stable at the SCF level.[23] Theoretical examinations of the growth mechanism, structural stability, and electronic structure of C_{28} were reported recently.[6,7,24] Kent et al.[25] used diffusion quantum Monte Carlo methods to study the energetic stability of a series of lower fullerenes ($n \leq 28$) and predicted C_{24} to be the smallest stable graphitic fragment and C_{28} the smallest stable fullerene.

The next higher fullerene C_{32} was found to be very stable with a huge mass signal. A large band gap,[9] comparable to the gap of C_{70}, indicates that C_{32} is the most stable fullerene for n < 60. Among the nine structural isomers of C_{32}, the cage structure with D_3 symmetry was found to be the most stable.[8] C_{36} is the smallest fullerene isolated up to now, and Piskoti et al.[26] first reported the synthesis of macroscopic quantities of C_{36}. A series of studies on the structure and bonding of charged and neutral species of C_{36} have been reported, where researchers confirm the D_{6h} triplet ground state as the most stable isomer of C_{36}.[27,28] C_{36} is highly reactive and possesses a strong tendency to form intermolecular covalent bonds, and it has large strain in the carbon skeleton.[28−30] Hydrogenated derivatives of C_{40} were first reported by Rohlfing et al.[31] C_{40} occurs in several symmetries, with D_{5d} thermodynamically most stable.[32]

The introduction of heteroatoms into C_{60} fullerenes is gaining interest due to significant changes in the structure and nature of the compound.[33−36] Doped fullerenes are believed to have wide applications due to their remarkable structural, electronic, optical, and magnetic properties.[37] Similar to C_{60}, lower heterofullerenes C_n (n < 60)[38,39] can be modified to increase the stability of these cage structures by altering their chemical composition. A number of recent studies have explored the possibility of formation of a stable structure of smaller fullerenes by substitutional doping. An investigation of the hydrogenation products and selected B-, N-, and P-doped analogues of smaller fullerenes C_n (n = 20−50) has been carried out by Chen et al.[40] at the B3LYP/6-31G* level of theory. The aromaticity and computed nucleus independent chemical shifts of the B-/N-doped C_{36} have been evaluated at the DFT level of theory.[41] Theoretical work on B- and N-substituted C_{40} indicated that the stability order of hetero-C_{40} is similar to that of hetero-C_{36}: $C_{40} > C_{38}B_2 > C_{38}BN > C_{38}N_2$.[42] The rise of the strain of heterofullerenes compared to that of the C_{40} cluster was noted. Theoretical prediction of B- and N-doped C_{40} fullerene has also indicated that doping can enhance the redox activity of C_{40}, similar to C_{60} [42] but different from that of C_{36}.[43]

However, little attention has been paid thus far to the smaller skeleton heterofullerenes as compared to n = 60 and 70 that are prepared in macroscopic quantities. B and N doping in these larger fullerenes follows certain rules,[44−46] such as heteroatoms prefer hexagon−hexagon (h−h) junctions over hexagon−pentagon (h−p) and the stability is enhanced by direct linking of B and N atoms. Since some of the lower fullerenes do not contain such hexagon−hexagon junctions, the question arises as to how BN units network in lower fullerenes as there are more variations of junctions with different bond lengths.[40] Although a few theoretical investigations[42,43] have been published on B- and N-doped smaller fullerenes, no systematic

* Address correspondence to this author. E-mail: tapaskar@cc.usu.edu. Fax: 1-435-797-3390. Phone: 1-435-797-7230.

10.1021/jp047833m CCC: $27.50
Published on Web 08/28/2004

TABLE 1: Relative Energies (E_{rel}), and CC and BN Bond Lengths of Doped Fullerenes

doped fullerenes	positions[a]			E_{rel} (kcal/mol)			R(CC) (Å)		R(BN) (Å)	
	B	N	junction[b]	MNDO	DFT[c]	DFT//MNDO[d]	MNDO	DFT[c]	MNDO	DFT[c]
$C_{18}BN$-1	1 (p)	3 (p)	p−p	0.00	0.00	0.00	1.408	1.422	1.542	1.518
$C_{18}BN$-2	1	17	Nc	4.53	14.98	15.38				
$C_{18}BN$-3	1	8	Nc	5.32	19.23	19.01				
$C_{18}BN$-4	1	19	Nc	5.67						
$C_{18}BN$-5	1	4	1−3	12.86						
$C_{22}BN$-1	15 (p)	21 (p)	p−p	0.00	2.37	0.00	1.388	1.365	1.502	1.464
$C_{22}BN$-2	15	19	Nc	6.74	18.55	19.19				
$C_{22}BN$-3	12 (p)	9 (p)	h−p	16.60	12.04	10.88	1.442	1.423	1.519	1.493
$C_{22}BN$-4	12 (h)	15 (p)	p−p	16.70	0.00	5.41	1.531	1.532	1.575	1.542
$C_{22}BN$-5	12	11	1−4	25.95	30.41	28.80				
$C_{22}BN$-6	15 (p)	12 (h)	p−p	35.60	25.86	26.00	1.531	1.532	1.587	1.514
$C_{26}BN$-1	2	8	1−3	0.00	6.58	6.47				
$C_{26}BN$-2	3 (h)	8 (p)	p−p	3.35	0.00	0.00	1.496	1.437	1.527	1.490
$C_{26}BN$-3	27 (p)	28 (p)	h−p	10.68	2.03	4.51	1.486	1.439	1.505	1.481
$C_{26}BN$-4	27	19	1−3	13.39						
$C_{26}BN$-5	20	8	Nc	16.24						
$C_{26}BN$-6	8 (p)	3 (h)	p−p	16.89	8.55	11.16	1.496	1.437	1.512	1.490
$C_{30}BN$-1	2 (h)	1 (p)	p−p	0.00	10.79	11.81	1.463	1.439	1.513	1.478
$C_{30}BN$-2	1 (p)	2 (h)	p−p	4.37	8.47	8.25	1.463	1.439	1.518	1.492
$C_{30}BN$-3	3 (p)	9 (p)	p−h	5.81	0.00	0.00	1.390	1.378	1.464	1.434
$C_{30}BN$-4	9 (p)	3 (p)	p−h	7.25	2.66	2.35	1.390	1.378	1.469	1.441
$C_{30}BN$-5	1	20	Nc	12.60						
$C_{30}BN$-6	17 (p)	18 (p)	h−h	21.57	13.20	13.06	1.449	1.454	1.500	1.511
$C_{34}BN$-1	32 (h)	29 (h)	p−p	0.00	0.71	1.01	1.509	1.491	1.534	1.530
$C_{34}BN$-2	17 (h)	32 (p)	p−h	7.20	0.00	0.00	1.448	1.431	1.505	1.488
$C_{34}BN$-3	17	18	1−3	11.24		5.79				
$C_{34}BN$-4	32 (p)	17 (h)	p−h	12.27	4.97	3.04	1.448	1.431	1.504	1.486
$C_{34}BN$-5	26 (p)	29 (p)	p−h	13.54	2.32	0.26	1.427	1.411	1.490	1.468
$C_{34}BN$-6	17 (p)	15 (p)	h−h	20.11	13.15	7.52	1.448	1.443	1.477	1.485
$C_{38}BN$-1	34 (p)	33 (p)	p−h	0.00	0.00	0.00	1.382	1.371	1.459	1.429
$C_{38}BN$-2	15 (p)	17 (p)	h−h	10.62	0.70	1.56	1.417	1.409	1.486	1.481
$C_{38}BN$-3	24 (h)	23 (p)	h−p	11.06	6.54	7.91	1.470	1.454	1.504	1.498
$C_{38}BN$-4	17 (p)	15 (p)	h−h	11.48	6.45	6.51	1.417	1.409	1.477	1.465
$C_{38}BN$-5	23 (p)	24 (h)	h−p	22.65	21.97	22.41	1.470	1.454	1.499	1.499
$C_{38}BN$-6	15 (h)	26 (h)	h−p	22.09	14.09	15.58	1.485	1.473	1.509	1.523
$C_{38}BN$-7	34 (h)	23 (h)	p−p	23.69	15.38	17.10	1.519	1.489	1.590	1.545

[a] See Figures 1 and 2 for the numbering schemes. p and h represent pentagon and hexagon, respectively. Participation in a hexagon or pentagon (besides the polygons involved in the B−N junction) is shown in parentheses. [b] Nc indicates the heteroatom pair are not connected to one another. 1−3 and 1−4 represent positions of unconnected heteroatoms in the same pentagon or hexagon. [c] B3LYP/6-31G*//B3LYP/6-31G*. [d] B3LYP/6-31G* energies at MNDO optimized geometry.

computational studies exploring BN isomers of small fullerenes have been reported.

The present investigation focuses on a MNDO and DFT study of mono-BN-substituted lower fullerenes C_n, where $n = 20$, 24, 28, 32, 36, and 40. In this series of fullerenes, the number of pentagons is constant at 12 with varying number of hexagons. It is expected that insertion of heteroatoms (B and N) in such structures may provide variations in the chemical stability and other properties as the size or the geometry of the cluster changes.[6] These properties might lead to nanoparticles with unusual intermolecular bonding and electronic properties. Hybrid BCN systems have already been an active field of research for several years as promising candidates for electronic devices.

Method of Calculation

Of the various semiempirical methods tested in our previous investigations,[45,46] MNDO predictions for the stability of C_{58}-BN fullerenes were found to be most consistent with more accurate methods such as B3LYP/3-21G//MNDO, B3LYP/3-21G//B3LYP/3-21G, B3LYP/6-31G*//B3LYP/3-21G, B3LYP/6-31G*//B3LYP/6-31G*, etc. On the basis of these findings, geometries of all systems were fully optimized by MNDO without any symmetry constraints. The energetically favored BN isomers, thus obtained, were subsequently optimized by using density functional theory (DFT), using B3LYP hybrid functionals[47,48] and the 6-31G* basis set. All calculations were performed with the Gaussian 98 program.[49] (Convergence problems were encountered with the 3-21G basis set for most of the doped fullerenes.)

Results and Discussion

In each group of BN-substituted C_n ($n = 20$, 24, 28, 32, 36, and 40), the relative energy (E_{rel}) of the most stable isomer (ground state) is set to zero; less stable isomers are arranged in increasing order of E_{rel} in Table 1 (according to MNDO). Several possible substitutions were examined in each fullerene, and the most favorable of these are listed in Table 1. To assess the reliability of MNDO results, the more reliable B3LYP/6-31G* method was used. As geometry optimization of fullerenes at the B3LYP/6-31G* level can be heavily time-intensive, E_{rel} values were also computed by B3LYP/6-31G*, using MNDO-optimized geometry to check the usefulness of such a protocol for stability estimation. Different isomers of doped fullerenes are depicted in Figures 1 and 2. Positions of carbon pairs undergoing BN substitution in each isomer are marked with an arrow for easy identification; bold numbers correspond to the

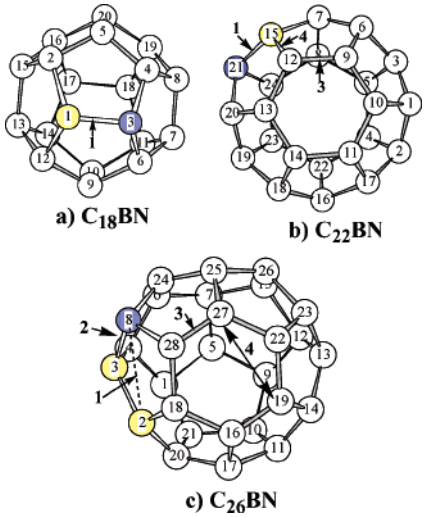

Figure 1. 3D diagrams of $C_{n-2}BN$ (n = 20, 24, and 28) fullerene isomers. Blue and yellow circles represent N and B atoms, respectively; all others are C atoms. Only the positions of the heteroatoms of the most stable isomer (**1**) are shown. Other isomers are marked by arrows with the same numbering scheme as in Table 1.

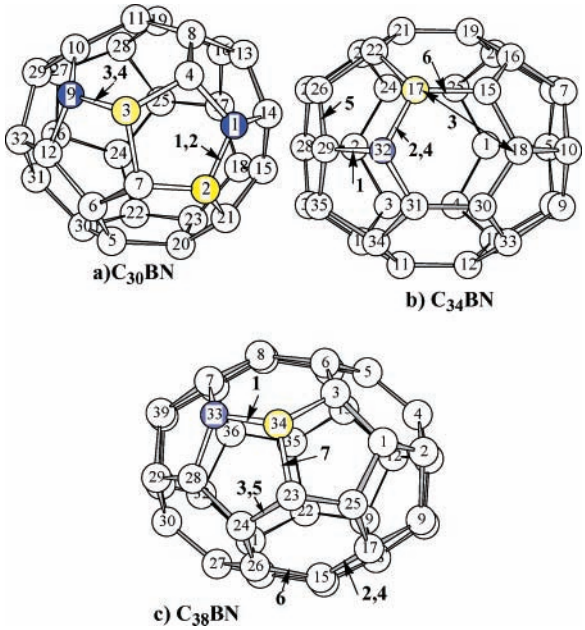

Figure 2. 3D diagrams of $C_{n-2}BN$ (n = 32, 36, and 40) fullerene isomers.

particular isomer in the first column of Table 1. Those marked with a 1 refer to the most stable geometry in each class.

A. Energetics and Substitution Patterns. *C_{20} fullerene*: C_{20} is the smallest fullerene possible with no hexagonal ring. It contains just 12 pentagons and is expected to be stabilized by electron correlation.[15] Several carbon pairs of the most stable C_2 symmetry[40] of the pure fullerene were replaced by B/N pairs and the five lowest energy isomers are listed in Table 1. CC replacement is preferred for any pair where B and N atoms are adjacent, e.g., the 1−3 pair where the CC bond length is the shortest (1.408 Å). In the other four listed isomers, B and N atoms are unconnected and spread over more than one pentagon: 1−17, 1−8, 1−19, and 1−4. Those isomers lie at least 4.5 kcal/mol higher in energy than the most stable one. The most stable structure of C_{20} is in good agreement with the rules established earlier for the larger $C_{58}BN$,[35,50−53] i.e., BN-fullerenes prefer adjacent B and N atoms. DFT calculation of the lowest three MNDO-optimized isomers (DFT//MNDO) reveals the trend is retained, but that the energy differences between the isomers are greatly enhanced. Note that reoptimization of the geometries by DFT leads to little further change.

C_{24} fullerene: The C_{24} (D_6) structure[19−22] introduces 2 hexagons along with 12 pentagons as shown in Figure 1b. Each hexagon is surrounded by six pentagons, and a new type of substitution site opens at the hexagon−pentagon (h−p) ring junctions. The DFT and MNDO C−C bond lengths of C_{24} lie in the ranges 1.365−1.532 and 1.388−1.531 Å, respectively. According to MNDO and DFT//MNDO, substitution at the shortest p−p junction (C_{15}−C_{21}) yields the preferred BN isomer (C_{22}BN-1 in Table 1). On the other hand, DFT optimization forgoes the "shortest bond length" rule for BN substitution: Isomer **1** is less stable by 2.4 kcal/mol than the 12−15 p−p junction substitution product **4**. Indeed, the 12−15 CC bond length in the unsubstituted C_{24} is the longest of all C−C bonds in that fullerene. It might be taken as a warning that this same isomer **4** would not be correctly treated by MNDO, which places it fully 16.7 kcal/mol higher in energy than **1**.

Both the 15−21 pair in isomer **1** and the 12−15 pair in **4** occupy adjacent positions in a single pentagon. Where they differ is in the other rings in which each atom participates. Atoms 15 and 21 participate in pentagons only (three pentagons each to be exact, designated p^3), whereas atom 12 participates in two pentagons and one hexagon (p^2h). The ideal angles for a pentagon and hexagon are of course 108° and 120°, respectively. Hence, stability might be expected to be enhanced by placing an atom that prefers larger angles in position 12. In general, the X−B−X angle in X_nBNY_n is wider than θ(Y−N−Y) as B and N atoms tend toward sp^2 and sp^3 hybridization, respectively. For example, the HNH angles are 5−6° smaller than θ(HBH) in H_3NBH_3; the corresponding difference in H_2NBH_2 is 8−9°. One may thus suppose that B would prefer to occupy a hexagon vertex, as compared to N. This guess is confirmed in that isomer **4**, where B is located at p^2h position 12, is in fact the most stable according to DFT. Reversing the positions of the B and N atoms of **4** leads to isomer **6**. DFT reveals that this simple reversal, which places N instead of B at a position where it must occupy a vertex of a hexagon, raises the energy by as much as 26 kcal/mol.

Comparison with isomer **1** uncovers useful information about MNDO as compared to DFT. As mentioned above, both substituted atoms in **1** lie at vertexes of pentagons only. The fact that MNDO predicts **1** to be nearly 17 kcal/mol more stable than **4** indicates that this semiempirical method places too much importance upon retaining not only N, but also B atoms, at pentagon positions. In summary, the most stable geometry, as calculated by DFT, places a N atom at a p^3 position, and B adjacent to it, at a p^2h site.

C_{28} fullerene: The tetrahedral structure of C_{28} is composed of 4 hexagons and 12 pentagons.[23,54] Each hexagon in the structure is connected to six pentagons; there are no direct hexagon−hexagon connections (Figure 1c). As shown in Table 1, MNDO predicts C_{26}BN-1 to be the most stable isomer, wherein the B and N atoms both occur in the same pentagon, and are separated by one C atom (2−8 positions). Such an arrangement contradicts previous findings of mono-BN-substituted fullerenes[44,45] where B and N atoms prefer to be directly connected. The second most stable isomer in the group is C_{26}BN-2, where the B and N atoms are in fact connected. DFT reverses this trend, conforming to the preference of contiguous B and N atoms, whether the MNDO geometry is DFT-reoptimized or not.

Isomer **6** is obtained by swapping the B and N atoms of $C_{26}BN$-2. The higher energy of **6** can be explained on the basis of strain. Atom 8 occupies a vertex of three different pentagons, whereas site 3 is involved with two pentagons and one hexagon. The larger angles required by the hexagon lead to the preference for B in site 3, and hence to the lower energy of **2**. In isomer **3**, both B and N occupy hexagonal positions (along with participation in two pentagons), but this structure is nonetheless only a few kilocalories per mole higher. As in the C_{24} case, the N atom prefers a site where it participates in pentagons only. The B atom prefers direct connection to this N, which places it at a site that participates in two pentagons and one hexagon.

C_{32} fullerene: The D_3 symmetry of the C_{32} species[8] contains 6 hexagons and 12 pentagons, providing for the first time a h−h junction (Figure 2a) where two hexagons meet. Mono-BN substitution is highly unfavorable at such a junction, as witness the high energy of structure **6**, which would involve sites 17 and 18, both of which are categorized as ph^2. The most stable DFT geometry of $C_{30}BN$ places B and N atoms at sites 3 and 9 (a p−h junction), respectively, which are both of p^2h type. In contrast, MNDO prefers sites 2 and 1, a p−p junction; these two sites are p^2h and p^3, respectively. The higher energy of this conformation **1** as compared to **3** via DFT represents the first occasion where the N atom forgoes occupation of a p^3 site in favor of p^2h.

The switching of B and N atoms between sites 3 and 9, which would yield structure **4**, is disfavored by some 2.5 kcal/mol. Both of these sites are of the p^2h variety, so the difference in energy might be attributed to the angles. The three angles around site 9 are 106°, 106°, and 120°, as compared to 108°, 109°, and 120° for site 3, explaining the preference of the B atom for the latter site, with its slightly larger angles. Comparison of structures **1** and **2** involves a similar switching of B and N atoms between a pair of sites. Whereas DFT favors the latter geometry, MNDO incorrectly favors the former. Although MNDO fails to comply with DFT trends, use of MNDO geometries does appear to provide a valid basis for applying DFT, thereby avoiding costly reoptimization of geometry.

C_{36} fullerene: The D_{6h} symmetry[27,28] of C_{36} contains 8 hexagons and 12 pentagons (Figure 2b) with three possible types of ring junctions (h−h, h−p, and p−p). BN occupation of a p−h junction in structure **2** is the most stable of those examined. The CC and BN bonds in this p−h junction (17−32) are significantly shorter than those of isomer **4** where the N and B atoms reverse places. This higher energy may be attributed in part to moving the N atom from a p^2h to a ph^2 position. MNDO calculations suggest **1** as the most stable structure, where B and N occupy a p−p junction. This situation represents a repetition of the C_{32} case where MNDO and DFT preferred p−p and h−p junctions, respectively.

C_{40} fullerene: There are 10 hexagons and 12 pentagons contained within the D_{5d} symmetry[32] of C_{40}. Both DFT and MNDO agree on the stability of geometry **1**, which places the B and N atoms at a p−h junction. Both $C_{34}-C_{33}$ and $B_{34}-N_{33}$ bonds are shortest in this isomer. The second most stable isomer **2** places the heteroatoms at a h−h junction; the CC and BN bonds are slightly longer than those in **1**. It might be noted that MNDO estimates a far greater energy difference between **1** and **2** than does DFT. Moving up further in energy, structures **3** and **5** situate B and N at a longer h−p junction. The preference for **3** over **5** is rooted in the placement of N at a p^2h rather than a ph^2 site in the former structure. Isomers where B and N atoms are not directly connected are much higher in energy; those results are not tabulated.

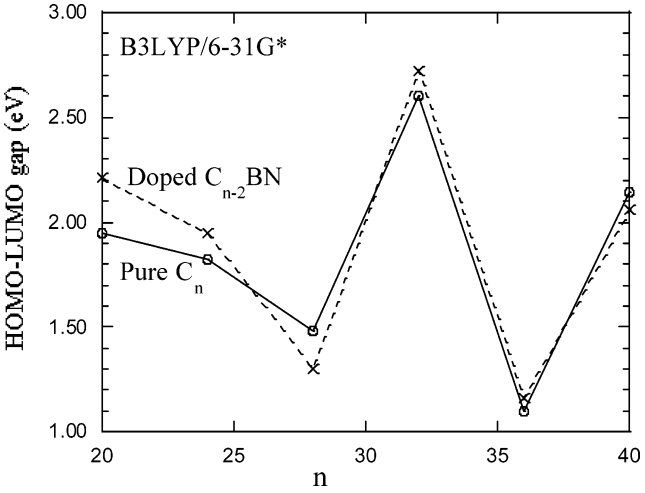

Figure 3. Variation of HOMO-LUMO gaps of pure and mono-BN-doped fullerenes with the total number of atoms.

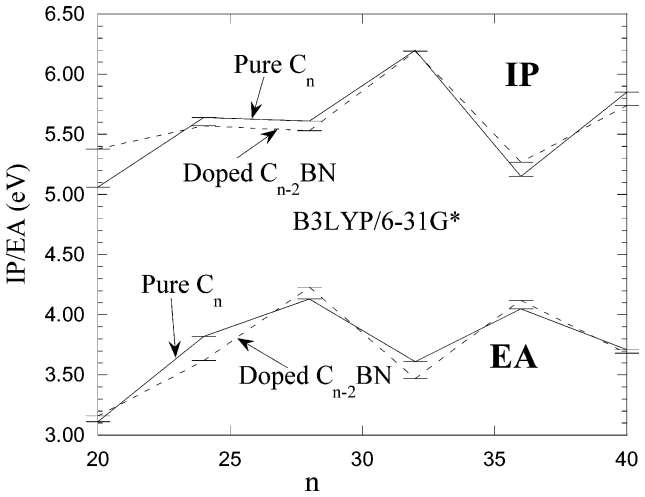

Figure 4. Variations of ionization potential (IP) and electron affinities (EA) of pure and mono-BN-doped fullerenes with the total number of atoms.

In summary, MNDO by itself exhibits a number of weaknesses in prediction of trends in relative energies. On the other hand, geometries optimized by MNDO are useful for single-point DFT calculations of energetics. The principle established earlier that B and N atoms tend to bond together in fullerenes is applicable to these smaller molecules as well. One factor contributing to the preferred positions of these BN pairs is the relevant bond lengths as the BN pair prefers shorter bonds, perhaps due to the B ← N dative bond. Another factor relates to the bond angles. Stability is enhanced by placing the N atom at a site with smaller bond angles, with B taking the alternate location with wider angles. This trend results in a preference of N for participation in pentagons and B in hexagons. A final principle noted (at the DFT level) is a preference of the BN pair for occupation of a p−h junction, when available, as opposed to a p−p junction.

B. HOMO-LUMO Gap, Ionization Potentials (IP), and Electron Affinities (EA). HOMO-LUMO gaps (closely related to band gaps) are traditionally associated with chemical stability against electronic excitations, with larger gaps corresponding to greater stability. Gaps of the most stable isomers of doped and undoped $C_{n-2}BN$ ($n \leq 40$) obtained from B3LYP/6-31G*//B3LYP/6-31G* are depicted in Figure 3. It is apparent that substitutional doping has a mixed influence on the HOMO-LUMO gap of lower fullerenes. It had been learned

earlier that mono-BN substitution of C_{60} lowers its gap by 0.22 eV. Both C_{28} and C_{40} also undergo a gap reduction upon BN substitution, by 0.18 and 0.08 eV, respectively. In contrast, the other smaller fullerenes show a gap widening upon replacement of a CC pair by BN. The largest change in this series, 0.26 eV, occurs in the highly strained C_{20}; the smallest increase of 0.06 eV is associated with C_{36}.

The ionization potentials (IPs) and electron affinities (EAs) of the pristine and doped C_n ($n \leq 40$) are compared in the upper and lower portions of Figure 4, respectively. There are no obvious systematic trends with regard to the effects of substitution. The maximum change of +0.32 eV (harder to oxidize) in IP is noted for $n = 20$, while for C_{32} the change is barely 0.01 eV. For $n = 24$, 32, and 40, doping eases reduction. The oscillation of IP and EA values of doped and pure fullerenes underscores the dependence of oxidation/reduction tendencies of heterofullerenes upon the number of atoms in the cage structure.

Conclusions

The most important factor for the stability of $C_{n-2}BN$ fullerenes is the connectedness of the heteroatoms, consistent with earlier findings for $C_{58}BN$. Another important factor resides in the CC and BN bond lengths. The BN group prefers replacement of a short CC bond. The CBC and CNC angles play a role as well, in that the N atoms tend toward smaller angles, leading them toward participation in pentagons over hexagons. Particularly as the cage is enlarged, one notices a preference of the BN pair of hexagon−pentagon over pentagon−pentagon junctions. While doping causes changes in the HOMO-LUMO gap, ionization potential, and electron affinity of pure fullerenes, no clear systematic trends have been identified. Although MNDO cannot be trusted to predict the most stable isomers, it does yield in most cases an adequate optimized geometry for application of the more reliable DFT method.

References and Notes

(1) Prinzbach, H.; Weiler, A.; Landenberger, P.; Wahl, E.; Worth, J.; Scott, L.; Gelmont, M.; Olevano, D.; BV, I. *Nature* **2000**, *407*, 60.

(2) Voytekhovsky, Y. L.; Stepenshchikov, D. G. *Acta Crystallogr., Sect. A*: *Found. Crystallogr.* **2001**, *A57*, 736.

(3) Raghavachari, K.; Strout, D. L.; Odom, G. K.; Scuseria, G. E.; Pople, J. A.; Johnson, B. G.; Gill, P. M. W. *Chem. Phys. Lett.* **1993**, *214*, 357.

(4) Saito, M.; Miyamoto, Y.; Okada, S. *Mol. Cryst. Liquid Cryst.* **2002**, *386*, 97.

(5) Gianturco, F. A.; Lucchese, R. R.; Sanna, N. *J. Chem. Phys.* **2003**, 118.

(6) Makurin, Y. N.; Sofronov, A. A.; Gusev, A. I.; Ivanovsky, A. L. *Chem. Phys.* **2001**, *270*, 293.

(7) Mishra, R. K.; Lin, Y.-T.; Lee, S.-L. *Int. J. Quantum Chem.* **2001**, *84*, 642.

(8) Sun, Q.; Wang, Q.; Yu, J. Z; Ohno, K.; Kawazoe, Y. *J. Phys.*: *Condens. Matter* **2001**, *13*, 1931.

(9) Kietzmann, H.; Rochow, R.; Gantefor, G.; Eberhardt, W.; Vietze, K.; Seifert, G.; Fowler, P. W. *Phys. Rev. Lett.* **1998**, *81*, 5378.

(10) Du, A. J.; Pan, Z. Y.; Huang, Z.; Li, Z. J.; Wei, Q.; Zhang, Z. X. *Appl. Phys.* **2002**, *16*, 3971.

(11) Kent, P. R. C.; Towler, M. D.; Needs, R. J.; Rajagopal, G. *Phys. Rev. B*: *Condens. Matter Mater. Phys.* **2000**, *62*, 15394.

(12) Yang, X. W.; Guichang; Yang, Z.; Shang, Z.; Cai, Z.; Pan, Y.; Wu, B.; Zhao, X. *THEOCHEM* **2002**, *579*, 91.

(13) Tomilin, F. N.; Avramov, P. V.; Varganov, S. A.; Kuzubov, A. A.; Ovchinnikov, S. G. *Phys. Solid State* **2001**, *43*, 973 (translation of Fizika Tverdogo Tela (Sankt-Peterburg)).

(14) Kroto, H. W. *Nature* **1987**, *329*, 529.

(15) Cioslowski, J. *Electronic structure calculations on fullerenes and their derivatives*; Oxford University Press: New York, 1995.

(16) Helden, G. V.; Hsu, T.; Gotts, N. G.; Kemper, P. R.; Bowers, M. T. *Chem. Phys. Lett.* **1993**, *204*, 15.

(17) Du, A. J.; Pan, Z. Y.; Ho, Y. K.; Huang, Z.; Zhang, Z. X. *Phys. Rev. B*: *Condens.Matter Mater. Phys.* **2002**, *66*, 035405/1.

(18) Ehlich, R.; Landenberger, P.; Prinzbach, H. *J. Chem. Phys.* **2001**, *115*, 5830.

(19) Jensen, F. *J. Chem. Phys.* **1998**, *108*, 3213.

(20) Martin, J. *Chem. Phys. Lett.* **1996**, *255*, 7.

(21) Raghavachari, K.; Zhang, B.; Pople, J. A.; Johnson, B. G.; Gill, P. M. W. *Chem. Phys. Lett.* **1994**, *220*, 385.

(22) Jensen, F. *Chem. Phys. Lett.* **1993**, *201*, 89.

(23) Guo, T.; Diener, M. D.; Chai, Y.; Alford, M. J.; Haufler, R. E.; McClure, S. M.; Ohno, T.; Weaver, J. H.; Scuseria, G. E.; Smalley, R. E. *Science* **1992**, *257*, 1661.

(24) Zhu, W. J.; Pan, Z. Y.; Ho, Y. K. *Surf. Coatings Technol. 2000* **2000**, *128*−*129*, 170.

(25) Kent, P. R. C.; Towler, M. D.; Needs, R. J.; Rajagopal, G. *Phys. Rev. B*: *Condens. Matter Mater. Phys.* **2000**, *62*, 15394.

(26) Piskoti, C.; Yarger, J.; Zettl, A. *Nature* **1998**, *393*, 771.

(27) Yuan, L. F.; Yang, J.; Deng, K.; Zhu, Q. S. *J. Phys. Chem. A* **2000**, *104*, 6666.

(28) Jagadeesh, M. N.; Chandrashakhar, J. *Chem. Phys. Lett.* **1999**, *305*, 298.

(29) Yuxue, L.; Shixuan, D.; Ruozhuang, L. *Carbon* **2002**, *40*, 2255.

(30) Yuan, L.; Yang, J.; Deng, K.; Zhu, Q. *J. Phys. Chem. A* **2000**, *104*, 6666.

(31) Rohlfing, E. A.; Lox, D. M.; Kalder, K. *J. Chem. Phys.* **1984**, *81*, 3322.

(32) Yang, X.; Wang, G.; Yang, Z.; Shang, Z.; Cai, Z.; Pan, Y.; Wu, B.; Zhao, X. *THEOCHEM* **2002**, *579*, 91.

(33) Guo, T.; Jin, C.; Smalley, R. E. *J. Phys. Chem.* **1991**, *95*, 4948.

(34) Miyamoto, Y.; Rubio, A.; Cohen, M. L.; Louie, S. G. *Phys. Rev. B* **1994**, *50*, 4976.

(35) Piechota, J.; Byszewski, P. Z. *Phys. Chem.* **1997**, *200*, 147.

(36) Chen, Z.; Jiao, H.; Hirsch, A.; Thiel, W. *J. Org. Chem.* **2001**, *66*, 3380.

(37) Xie, R.-H.; Bryant, G. W.; Jensen, L.; Zhao, J.; Smith, V. H., Jr. *J. Chem. Phys.* **2003**, *118*, 8621.

(38) Shellmov, K. B.; Clemmer, D. E.; Jarrold, M. F. *J. Chem. Soc., Dalton Trans.* **1996**, 567.

(39) Strout, D. L. *J. Phys. Chem. A* **2001**, *105*, 261.

(40) Chen, Z.; Jiao, H.; Buhl, M.; Hirsch, A.; Thiel, W. *Theor. Chem. Acc.* **2001**, *106*, 352.

(41) Chen, Z.; Jiao, H.; Hirsch, A.; Thiel, W. *Chem. Phys. Lett.* **2000**, *329*, 47.

(42) Yang, X.; Wang, G.; Shang, Z.; Pan, Y.; Cai, Z.; Zhao, X. *Phys. Chem. Chem. Phys.* **2002**, *4*, 2546.

(43) Yang, Z. Y.; Xu, X. F.; Wang, G. C.; Shang, Z. F.; Cai, Z. S.; Pan, Y. M.; Zhao, X. Z. *J. Mol. Struct. (THEOCHEM)* **2002**, *618*, 191.

(44) Pattanayak, J.; Kar, T.; Scheiner, S. *J. Phys. Chem. A* **2001**, *105*, 8376.

(45) Pattanayak, J.; Kar, T.; Scheiner, S. *J. Phys. Chem. A* **2002**, *106*, 2970.

(46) Kar, T.; Pattanayak, J.; Scheiner, S. *J. Phys. Chem. A* **2003**, 107, 8630.

(47) Becke, A. D. *J. Chem. Phys.* **1992**, *96*, 2155.

(48) Becke, A. D. *J. Chem. Phys.* **1993**, *98*, 5648.

(49) Frisch, M. J.; Trucks; H. B.; Schlegel, G. W.; Scuseria, G. E.; Robb, M. A.; Cheeseman, J. R.; Zakrzewski, V. G.; Montgomery, J. A.; Stratmann, R. E.; Burant, J. C.; Dapprich, S.; Millam, J. M.; Daniels, A. D.; Kudin, K. N.; Strain, M. C.; Farkas, O.; Tomasi, J.; Barone, V.; Cossi, M.; Cammi, R.; Mennucci, B.; Pomelli, C.; Adamo, C.; Clifford, S.; Ochterski, J.; Petersson, G. A.; Ayala, P. Y.; Cui, Q.; Morokuma, K.; Malick, D. K.; Rabuck, A. D.; Raghavachari, K.; Foresman, J. B.; Cioslowski, J.; Ortiz, J. V.; Baboul, A. G.; Stefanov, B. B.; Liu, G.; Liashenko, A.; Piskorz, P.; Komaromi, I.; Gomperts, R.; Martin, R. L.; Fox, D. J.; Keith, T.; Al-Laham, M. A.; Peng, C. Y.; Nanayakkara, A.; Gonzalez, C.; Challacombe, M.; Gill, P. M. W.; Johnson, B.; Chen, W.; Wong, M. W.; Andres, J. L.; Gonzalez, C.; Head-Gordon, M.; Replogle, E. S.; Pople, J. A. *Gaussian 98*, Revision A.7; Gaussian, Inc.: Pittsburgh, PA, 1998.

(50) Shkrabo, D. M.; Krasyukov, Y. N.; Mukhtarov, E. I.; Zhizhin, G. N. *J. Struct. Chem.* **1998**, *39*, 323.

(51) Esfarjani, K.; Ohno, K.; Kawazoe, Y.; Gu, B. L. *Solid State Commun.* **1996**, *97*, 539.

(52) Esfarjani, K.; Ohno, K.; Kawazoe, Y. *Phys. Rev. B* **1994**, *50*, 17830.

(53) Esfarjani, K.; Ohno, K.; Kawazoe, Y. *Surf. Rev. Lett.* **1996**, *3*, 747.

(54) Portmann, S.; Galbraith, J. M.; Schaefer, H. F.; Scuseria, G. E.; Luthi, H. P. *Chem. Phys. Lett.* **1999**, *301*, 98.